

Simulation of the seasonal evolution of macroalgae in the lagoon of Venice

C. Solidoro, V.E. Brando, D. Franco, R. Pastres, G. Pecenic and C. Dejak

Department of Physical Chemistry, Section of Ecological Physical Chemistry, University of Venice, Dorsoduro 2137, I-30123 Venice, Italy
E-mail: cosimo@unive.it

A 3D reaction-diffusion model is presented, which describes the dynamics of two communities of primary producers, phytoplankton and macroalgae, and their effects on the oxygen balance in the lagoon of Venice. The model includes ten state variables: zooplankton, phytoplankton and *Ulva rigida* densities, nitrogen concentration in Ulva (quota), ammonium, nitrate and orthophosphate concentration in water, detritus, dissolved oxygen and water temperature.

The spatial distribution of Ulva shows a well defined pattern, also with homogeneous initial conditions. Such distributions become closer to the real ones when the initial conditions for Ulva are obtained by processing remote sensing data. The massive presence of Ulva greatly affects the DO balance, as hypoxic crises occur in the core of Ulva colonies in the early morning, as a consequence of respiration.

1. Introduction

The modification of the ecological conditions in the lagoon of Venice [9] has prompted the introduction of macroalgae dynamics in a 3D finite-difference model. The model, which was originally developed to assess the environmental impact of a power plant, has been gradually improved for analysing eutrophication in the lagoon of Venice and its effects on water quality [4,6]. The grid covers the central part of the Venice lagoon, which includes the most important industrial area of Porto Marghera and the city of Venice. This area is discretized on a mesh of 100 m by 100 m with a vertical step of 1 m, in order to solve numerically the following equation:

$$\partial \mathbf{c}(x, y, z, t) / \partial t = \nabla (\mathbf{K}(x, y, z) \nabla \mathbf{c}(x, y, z, t)) + \mathbf{f}(x, y, z), \quad (1)$$

where \mathbf{c} is the state vector, \mathbf{K} the eddy-diffusivity tensor and \mathbf{f} the local reaction term.

The transport term includes only the turbulent diffusion. The advection has not been considered explicitly, as the residual currents in the Venice lagoon have a marginal influence [1,4]. Nevertheless, the eddy-diffusivity tensor \mathbf{K} embodies the average effect of the tidal agitation, as it has been computed on the basis of a representative velocity field [2]. As a result, the diffusivity coefficients vary in accordance with the local hydrodynamics characteristics [1,2].

The system exchanges energy and matter through its open boundaries. Water temperature is included as a state variable, because it varies according with the bathymetry. This variable is driven by the energetic inputs at the air-water interface, based on averaged daily meteorological data [3]. The same data set has also been used to estimate the average daily light intensity for photosynthesis, which has been partitioned within each day to simulate the night-day cycle. Nutrients are immitted from point (industrial

area, rivers) and non-point sources (the sewage of the city of Venice, the major islands and atmospheric deposition). Outward fluxes through the horizontal open boundaries are computed by a specifically designed algorithm [4].

2. Modelling of macroalgae dynamics

The inclusion of macroalgae dynamics in the model has required the introduction of new state variables and processes, which were selected after a careful analysis of the literature and of the existing field and laboratory data [12,13]. Extensive field investigations show that *Ulva rigida* is, by far, the most abundant macroalgae in the Venetian ecosystem [8,10]. Its growth follows a two-step kinetic, uncoupling growth from assimilation. This feature forces one to introduce also the internal concentrations of nutrients as state variables, along with Ulva densities. As phosphorous seldom limits Ulva growth, the internal storage has been defined only for nitrogen and called Q (Quota). The influence of light and temperature on the specific growth rate and respiration has been described by asymptotic formulations, as this species tolerates high temperatures and solar radiation levels [13].

Due to their size, macroalgae can certainly not be treated as passive tracers, as is done for the other state variables. Up to now, there has been no quantitative information on the dispersion of Ulva colonies and, therefore, their expansion during the good season had to be modelled on purely empirical assumptions. Macroalgae are confined to the bottom layer and their diffusion along both horizontal directions is described by a single diffusivity D_U . This coefficient is empirical, and has been tuned by a visual comparison of the space distributions obtained by the model and the observed ones. The survival of macroalgae in a newly colonised area depends on D_U , on the trophic state of the

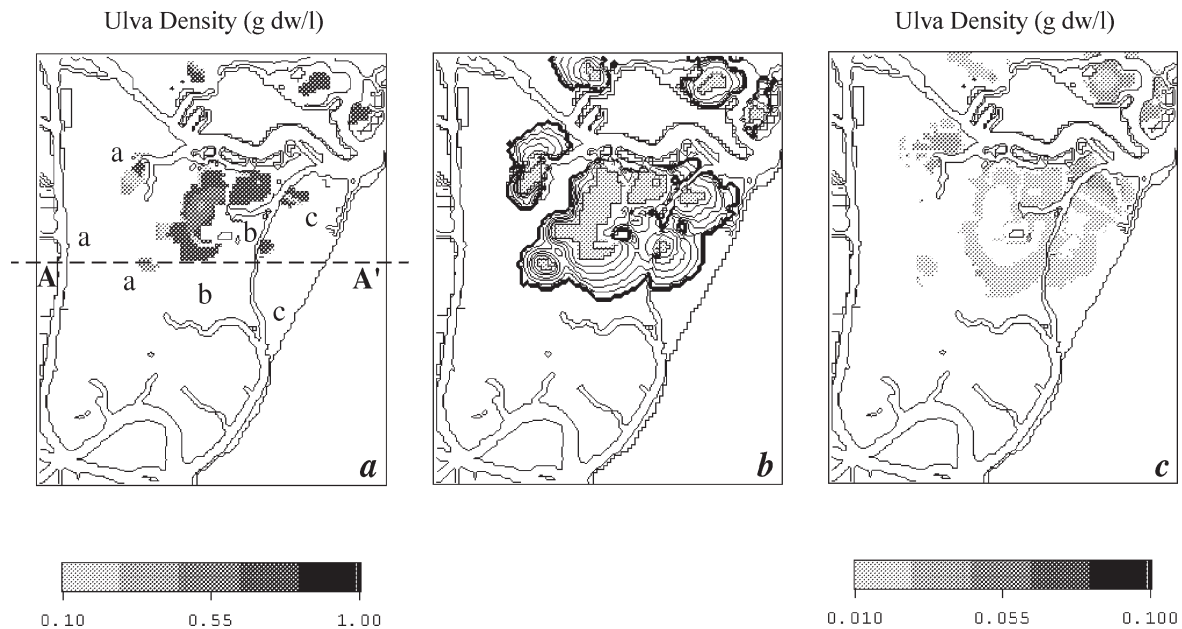


Figure 1. Initial distribution of *Ulva r.*, estimated from remote sensing data (a), dynamics of its yearly evolution (b) and distribution reached after the winter (c). The spreading of *Ulva* colonies from day 147 to 273 in (b) is illustrated by the lines, drawn every 21 days, that contour the area in which *Ulva* density is greater than 1 kg ww/m^2 . The three main areas colonized by macroalgae are labelled 'a', 'b', 'c' in figure 1a.

area and on the bathymetry. This is in agreement with the experimental observations, which show the presence of *Ulva r.* only in well defined areas.

The zooplankton-phytoplankton dynamics has already been described in a previous paper [12]. According to formulations quite commonly adopted [5], the dependence of the specific growth rate of phytoplankton on the concentration of external nutrients, N and P, is modelled by a Monod kinetic. The influence of the water temperature is accounted for by a Lassiter–Kearns function, characterized by an optimum temperature, while a Steel formulation, which takes photoinhibition into account, is used for describing the influence of light intensity on growth rate. Zooplankton grazing follows a type II functional response, while linear terms describe mortality losses. Nutrient regeneration is described through the dynamics of two state variables, namely detritus and surface sediment. Mortality losses enter the detritus compartment (labile fraction of dead organic matter); detritus sinks at a constant rate and, eventually, reaches the bottom, where it is transferred to the surface sediment compartment. Remineralization takes place both in the water column and in the surface sediment, releasing nutrient back to the water medium. The rate of these processes depends in the same way on oxygen availability as well as on water temperature.

Phytoplankton and macroalgae compete indirectly for the available nutrients, which are partitioned according to the ratio of the two biomasses, when the resources are limited. On the contrary, there is a direct competition for light, since phytoplankton, which remains on the top of the water column, partially shades the macroalgae community, usually weakly attached to the bottom.

The oxygen balance is very complex, as it is the result

of many processes: phytoplankton and macroalgae production and respiration, the degradation of organic matter in the detritus or sediment compartments, and reaeration. When dissolved oxygen falls below a certain threshold, the condition of the ecosystem becomes critical. This feedback is mathematically described by increasing the mortality of algae in proportion to the difference between the oxygen demand exerted by respiration of *Ulva r.*, and the availability of dissolved oxygen. This difference represents the fraction of biomass that can not respire and is likely to be damaged [13].

3. Results and discussion

The consistency of the model has been tested first at a qualitative level, to verify its capacity to reproduce the spatial pattern of *Ulva rigida*, starting from a homogeneous initial condition. The yearly evolution of the model shows that *Ulva* successfully outcompetes phytoplankton in the shallower areas, where the light intensity reaching the bottom can sustain its growth efficiently. In some of these areas, nutrient concentration becomes limiting, but the main factor in the competition appears to be the availability of light, which seems to give a selective advantage to *Ulva r.*, which grows more efficiently at lower light intensities. Vertical discretization turns out to be very important, because it permits a realistic description of shading and selfshading and puts in evidence the effect of the vertical gradients of nutrients and DO.

The spatial distributions become more realistic by setting the initial condition for *Ulva r.* according to the map of *Ulva* density shown in figure 1a, estimated by superimposing the grid of the model onto a remote sensing image, pre-

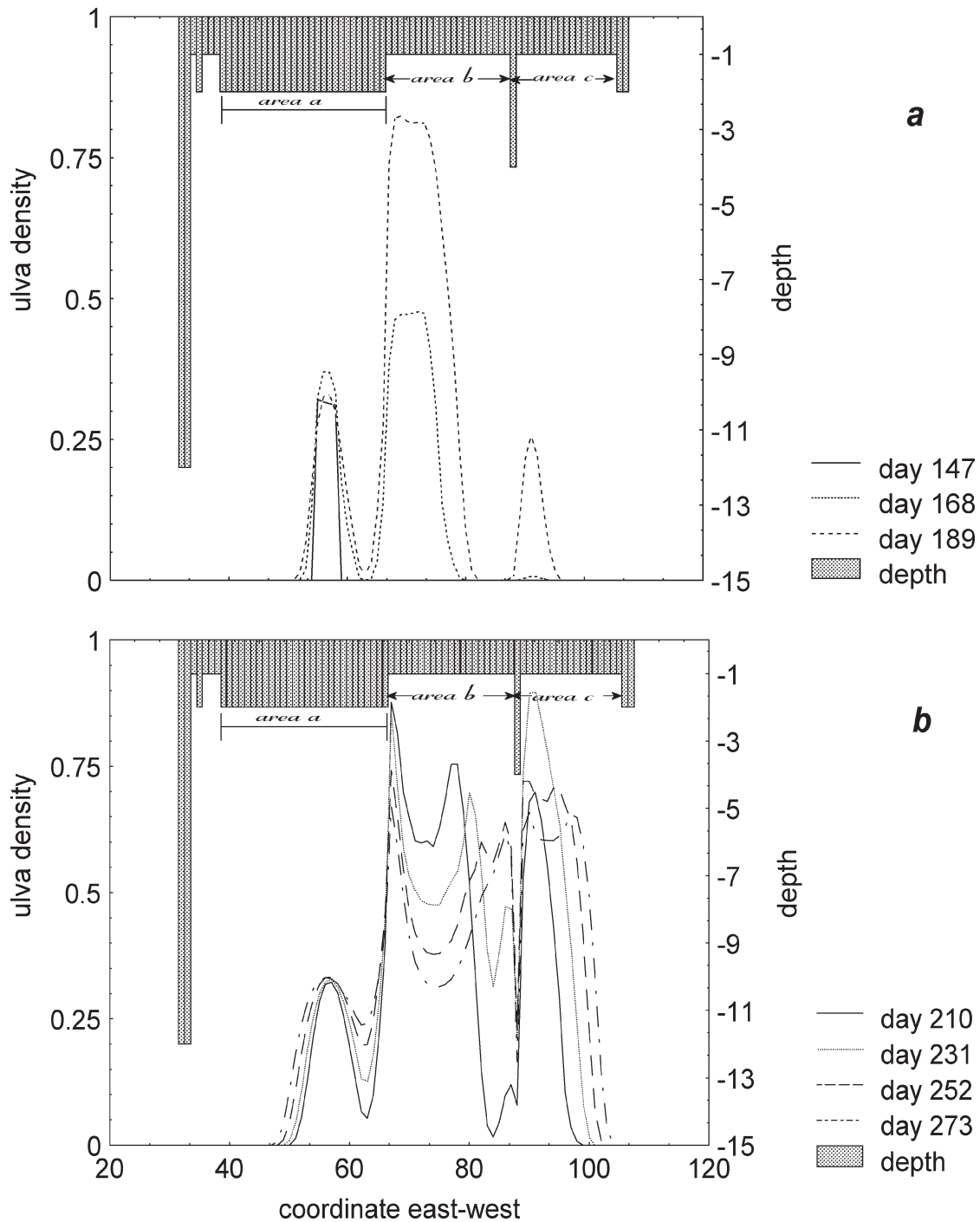


Figure 2. Biomass density along the section A-A', indicated in figure 1a, on day 147, 168, 189 (a) and on day 210, 231, 252, 273 (b).

processed as in [11]. The spreading of macroalgae colonies is illustrated in figure 1b: the contour lines are drawn every three weeks, starting from the initial distribution of figure 1a and show the larger and larger areas in which Ulva density is greater than 1 kg/m^2 (wet weight). Around the end of September, the expansion is stopped by climatic conditions and the colonies start contracting, reaching the distribution shown in figure 1c around the middle of February.

Figures 2a and 2b show the expansion of macroalgae colonies at the section A-A' of figure 1a, by comparing

biomass density on the same days for which the contour lines are drawn. At the beginning, day 147 in figure 2a, there is only one peak (solid line), because Ulva is present only in the region 'a'. After 21 days (dotted line), the first peak is broader, and another one arises as a consequence of the invasion of macroalgae from area 'b'. Then, at day 189, peak 'a' becomes flatter, while biomass density in the region 'b' increases up to 0.9 kg dw/m^2 , that is about 10 kg ww/m^2 . Peaks 'a' and 'b' increase at different rates, because area 'a' is deeper than 'b', as can be checked by

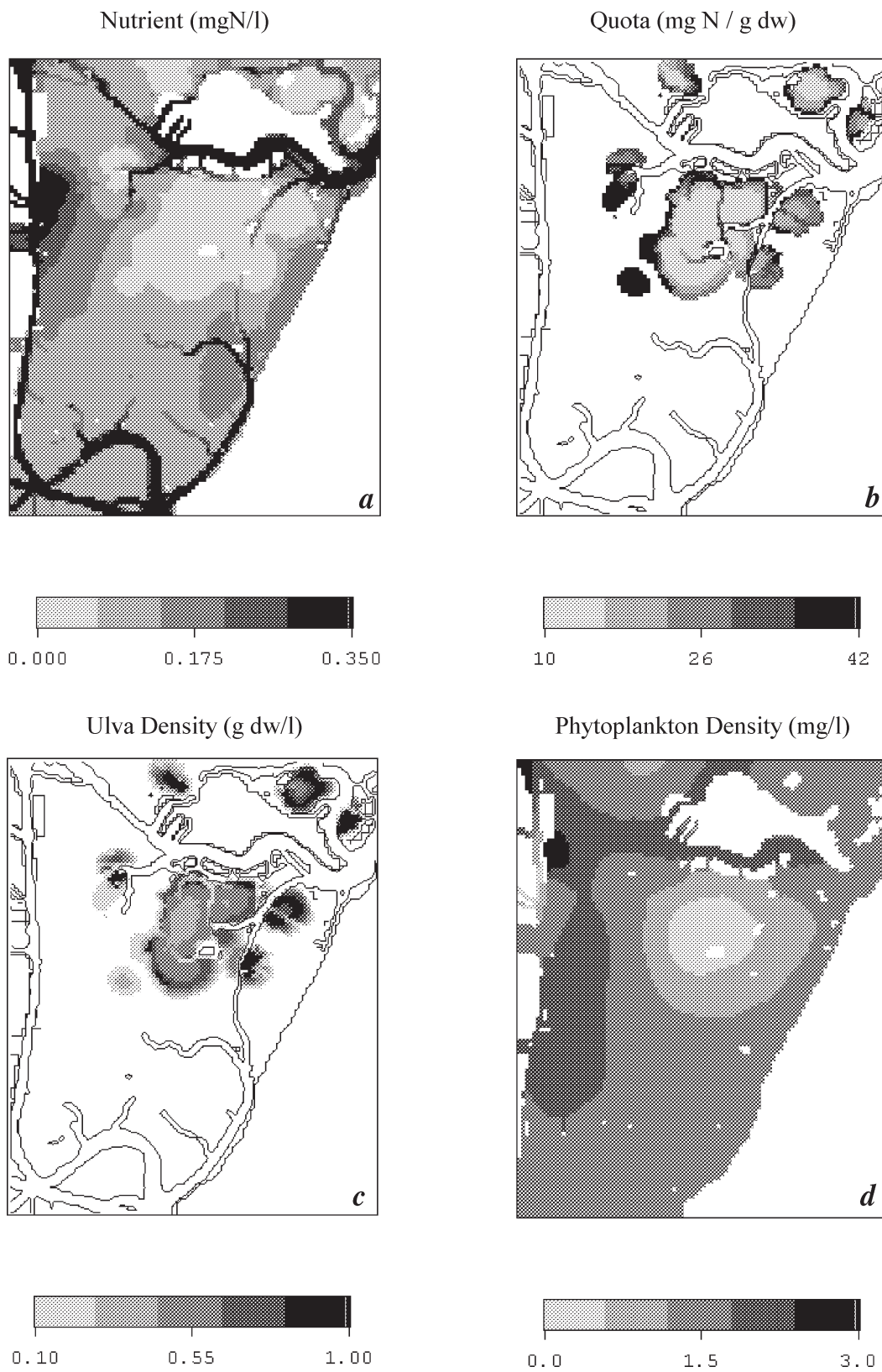


Figure 3. Spatial distributions of nutrient concentration (a), Quota (b), Ulva biomass (c), and phytoplankton density (d), on day 210.

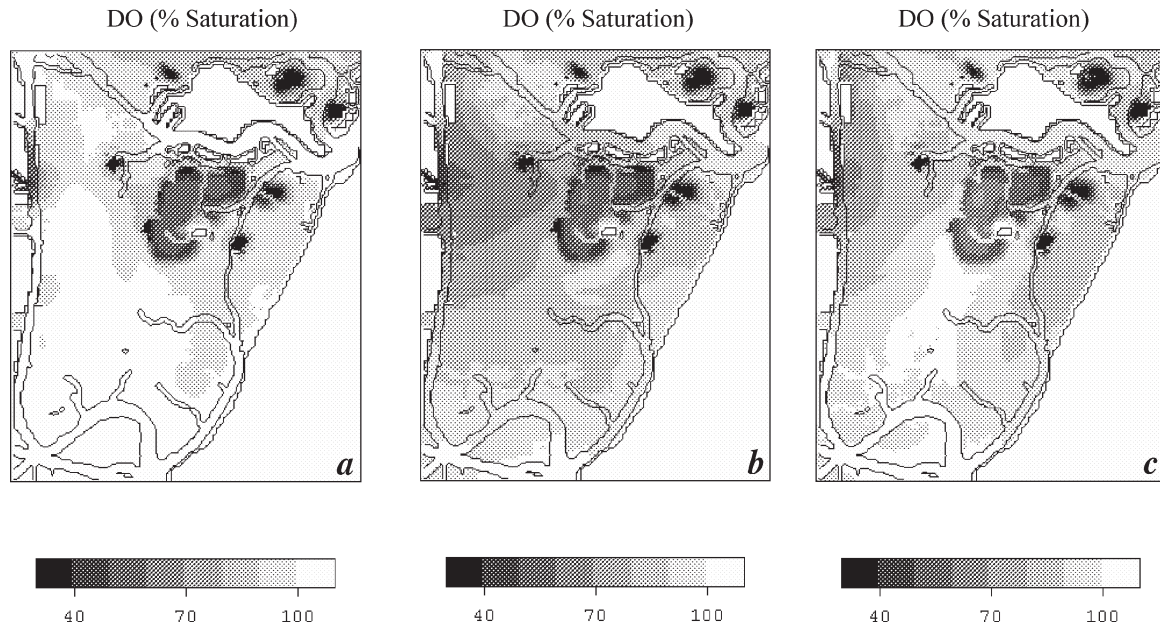


Figure 4. Maps of dissolved oxygen concentrations for days 185 (a), 190 (b), 195 (c) of the simulated year.

looking at the depth along the section, reported at the top of the figure. This difference explains why the two peaks remain separate. Peak 'c', which is barely noticeable at day 168, becomes evident at day 189, as a consequence of the expansion of colonies in area 'c', which is shallow and close to a channel. This channel keeps peaks 'b' and 'c' separate, bringing nutrients to these areas. The evolution of the colonies during the full summer is shown in figure 2b. *Ulva* biomass reach higher values at the edge of the colonies, as indicated by the splitting of peak 'b' into two parts. This evolution can be explained by the lack of nutrients in the core of the colony. In fact, colony 'b' receives nutrient supplies from the surroundings, and, as a consequence, its two external edges are richer in nutrients than its core. Moreover, the edges act as a barrier for nutrients, which are mostly assimilated there. This trend, which is frequently observed in our simulations, can be seen in the later profiles in figure 2b, which show a marked depression of the core of the colony as time goes on. As the simulation proceeds, the two colonies 'a' and 'b' are almost merged, while the presence of a deep channel between 'b' and 'c' is reflected by the two distinct peaks.

The maximum density in area 'c' is reached on day 252, in area 'b' on day 210 and area 'a' on day 168: this is in agreement with the phases of colonization and suggests that during this period there are good conditions for algae growth. Finally, the last profile, day 273, indicates also the splitting of peak 'c'.

This typical evolution of the algal colonies is consistent with the spatial distribution of nutrient concentration and quota, as shown in figures 3a and 3b, both referring to day 210. One can see that nutrient concentration is higher along the channels and the internal nitrogen, Quota, is lower in the middle of the *ulva* colonies, see figure 3c, where growth is limited. The distribution of phytoplankton density, fig-

ure 3d, shows, instead, that the abundance of this community, which is subjected to a space-dependent diffusion process, is not correlated to the bathymetry. Its density is lower where *Ulva* is present, since macroalgae is more efficient in uptaking dissolved nutrients, but phytoplankton blooms quickly after *Ulva* decays.

Dissolved oxygen is close to the saturation value along the major channels and above it in concomitance with algae blooms. In the shallow areas, *Ulva* respiration and bacterial mineralization cause the depletion of DO, whose concentration becomes extremely low in the core of *Ulva* colonies, above a certain level of biomass. If reaeration cannot restore the oxygen balance overnight, this situation can persist in the bottom layers, close to the sediment, where photosynthetic activity is reduced by nutrient depletion and self-shading effects. Since the lack of oxygen has a feedback effect on the rate of *Ulva* mortality, the oxygen demand for mineralization further increases. In these conditions, a local anoxia can cause a general dystrophic crisis: the population of *Ulva* suddenly collapses and the phytoplanktonic pool can take advantage of the large release of nutrients, until the macroalgae recover from the crisis. During the crisis, benthic regeneration becomes the most important source of nutrients in the core of the colonies, where it accounts for up to 70% of the total. The evolution outlined above is illustrated by figure 4, which shows the spatial distribution of DO at the beginning, figure 4a, in the middle, figure 4b, and towards the end, figure 4c, of an anoxic crisis.

The effects of different scenarios of incident light, nutrient load, or rate of expansion of *Ulva*, have been studied in other simulations. The results are summarized in figure 5, in which the number of cells occupied by *Ulva* (5a), the total *Ulva* biomass, computed over the area covered by the model (5b), and the maximum value of biomass observed in the area covered by the model (5c) are plotted versus time.

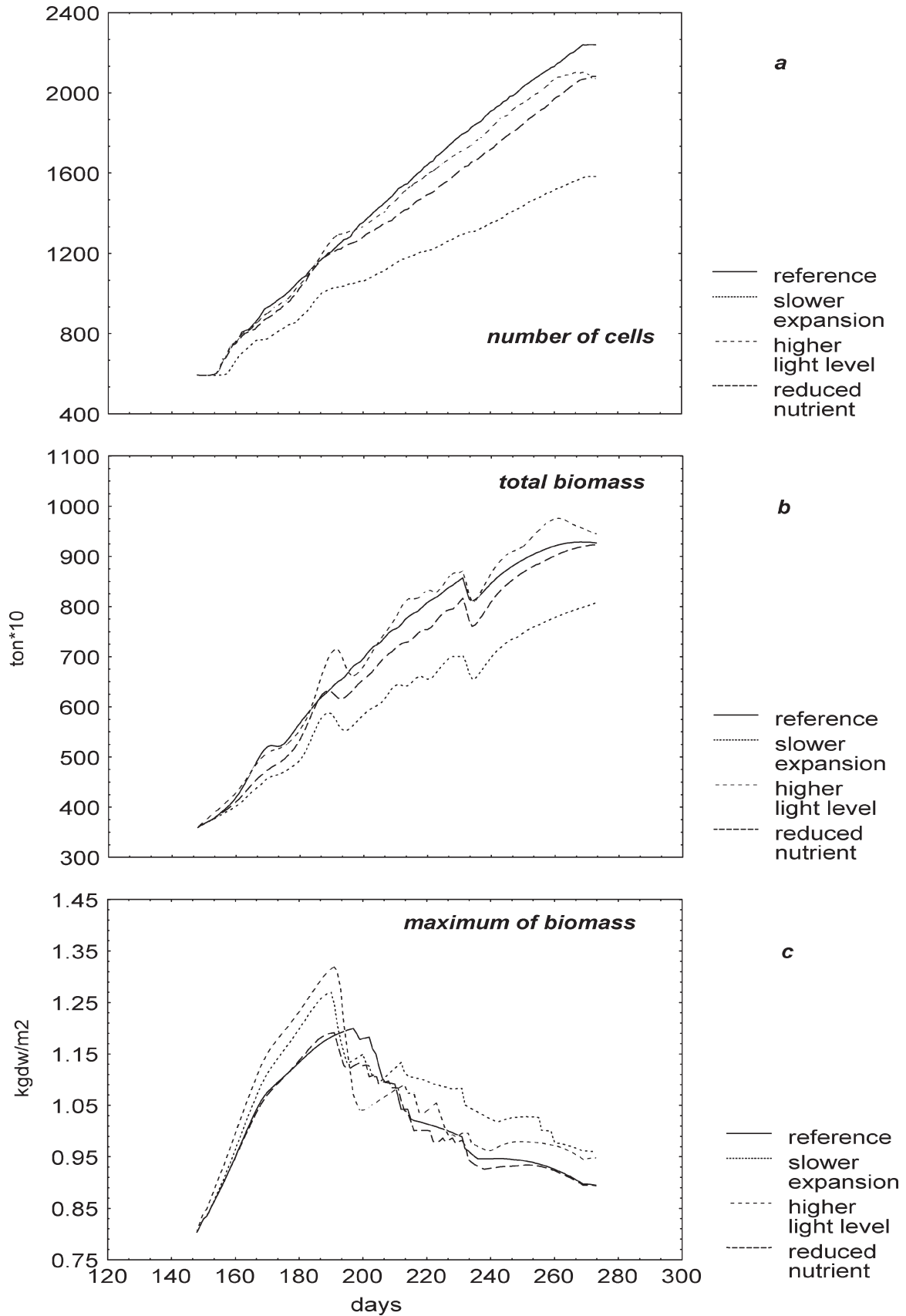


Figure 5. Time evolution of: number of cells occupied by Ulva (a), total Ulva biomass, computed over the area covered by the model (b), and maximum value of biomass observed in the area covered by the model (c).

The area colonised is smaller than in the reference simulation, if the rate of expansion is reduced, as can be noticed from figure 5a. A reduced expansion rate lowers the total biomass, as can be seen from figure 5b, but the accumulation of biomass causes an increase in the maximum value, see figure 5c.

A halving of the nutrient load does not change the spatial distribution of *Ulva r.* appreciably, but the limitation on growth can be noticed in figure 5: the dashed line always lies below the continuous one, which represents the reference simulation.

A higher level of incident light, 130% of the reference, does not affect the spatial distribution either. Nevertheless, standing crop values are significantly higher than in the reference simulations (figure 5b, narrow dotted line), indicating that this scenario is more favourable for *Ulva* growth. This supports the hypothesis that light availability is a limiting factor in the reference simulation.

The above results show that this model, by describing both transport processes and ecological dynamics, is a useful tool for understanding the spatio-temporal evolution of a complex system. However, it could also be used for orienting an environmental policy, as it can provide, at least, qualitative information on the modification induced by changes of the external conditions (i.e., nutrient loads, temperature, etc.) and can help in assessing remediation activities. Its use as a management tool would require more attention to the quantitative agreement with the observations and a sensitivity/uncertainty analysis of model results, in order to assess the confidence of the output. These issues are currently being investigated as part of other research projects, which have already achieved interesting results [7,14].

4. Conclusion

The yearly evolution of the model, under different environmental scenarios, shows that the spatial distribution of *Ulva r.* is strongly affected by bathymetry. In fact, *Ulva* colonies survive only in areas less than two meters deep, probably because below this depth, the solar radiation reaching the bottom is too low in an environment characterised by high turbidity.

Availability of nutrient is also a limiting factor for *Ulva* growth, which causes a spatial differentiation within the colony. In favourable conditions, a colony increases its total biomass and spreads until it is so large that the uptake at the edges markedly reduces the amount of nutrients reaching the core. In this way, the algae growing on the edge prevail in the intraspecific competition for nutrients. Further, *Ulva* growth is favoured in the shallow areas closer to the main channels, which guarantee a supply of nutrients.

Local anoxia can end in a general dystrophic crisis, when reaeration cannot provide the oxygen required for *Ulva* respiration and mineralization of detritus: since the lack of oxygen has a feedback effect on the rate of *Ulva* mortality, the oxygen demand for mineralization further increases, causing a sudden collapse in the population of *Ulva*.

References

- [1] C. Dejak, D. Franco, R. Pastres and G. Pecenic, A 3D eutrophication-diffusion model of the Venice Lagoon: some applications, in: *Residual Currents and Long-term Transport*, ed. R.T. Cheng, Coastal and Estuarine Studies 38 (1990) pp. 526–538.
- [2] C. Dejak, D. Franco, R. Pastres, G. Pecenic, I. Polenghi and C. Solidoro, 3D modelling of water quality transport process with time and space varying diffusivity tensors, in: *Proceedings of IUTAM 1995*, University of Western Australia, Perth (September 1995).
- [3] C. Dejak, D. Franco, P. Pastres, G. Pecenic and C. Solidoro, Thermal exchanges at air-water interfaces and reproduction of temperature vertical profiles in water columns, *Jour. Marine Systems* 3 (1992) 465–476.
- [4] C. Dejak and G. Pecenic, Special issue: Venice lagoon, *Ecol. Modelling* 37(1/2) (1987) 1–101.
- [5] G.T. Orlob, *Mathematical Modeling of Water Quality: Streams, Lakes and Reservoirs* (Wiley, Chichester, 1983).
- [6] R. Pastres, D. Franco, G. Pecenic, C. Solidoro and C. Dejak, Using parallel computers in environmental modelling: a working example, *Ecol. Modelling* 80(1) (1995) 69–86.
- [7] R. Pastres, D. Franco, G. Pecenic, C. Solidoro and C. Dejak, Local sensitivity analysis of a distributed parameters water quality model, *Reliability Engineering and System Safety* (in press).
- [8] A. Sfriso, Flora and vertical distribution of macroalgae in the lagoon of Venice: a comparison with previous studies, *Giornale botanico italiano* 121 (1987) 69–85.
- [9] A. Sfriso, A. Marcomini and B. Pavoni, Relationship between macroalgal biomass and nutrient concentrations in a hypertrophic area of the Venice Lagoon, *Mar. Envir. Res.* 22 (1987) 297–312.
- [10] A. Sfriso, B. Pavoni and A. Marcomini, Macroalgae and phytoplankton standing crops in the central Venice Lagoon: primary production and nutrient balance, *The Science of Tot. Envir.* 80 (1989) 139–159.
- [11] C. Solidoro, E.V. Brando, C. Dejak, D. Franco, R. Pastres and G. Pecenic, Remote sensing as a tool for 3D model of ecosystem: an application to the lagoon of Venice, in: *Proceedings of the Int. Conference on Computer Techniques in Environmental Studies VI*, ed. P. Zannetti (Springer, Berlin, Computational Mechanics Pub., Southampton, 1996) pp. 427–436.
- [12] C. Solidoro, C. Dejak, D. Franco, R. Pastres and G. Pecenic, A model for macroalgae and phytoplankton growth in the Venice Lagoon, *International Environment* 21(5) (1995) 619–626.
- [13] C. Solidoro, C. Dejak, G. Franco, R. Pastres and G. Pecenic, Modelling macroalgae (*Ulva rigida*) in the Venice Lagoon: model structure identification and first parameters estimation, *Ecol. Modelling* (in press).
- [14] C. Solidoro, R. Pastres, D. Franco, G. Pecenic and C. Dejak, Sensitivity analysis of an eutrophication model for shallow water environments colonized by *Ulva r.*, *Journal of Analytical and Environmental Chemistry* 86 (1996) 677–684.